Ionospheric electron concentration effects on SAR and INSAR

Urs Wegmüller, Charles Werner, Tazio Strozzi, and Andreas Wiesmann
Gamma Remote Sensing, Worbstrasse 225, CH-3073 Gümligen, Switzerland
http://www.gamma-rs.ch e-mail: wegmuller@gamma-rs.ch

Abstract —The launch of ALOS and the high potential expected for the L-band PALSAR motivated us to investigate ionospheric electron concentration effects using JERS L-band SAR data acquired at high latitudes. An important focus of our work was on the identification of ionospheric effects and resulted in methodologies to detect ionospheric effects in single SAR acquisitions as well as in repeat-orbit pairs. For cases where significant ionospheric anomalies are present, procedures to improve SAR offset tracking and interferometric results are proposed and the retrieval of free electron density maps is discussed.

Keywords: Ionosphere, L-band SAR, JERS, ALOS PALSAR, azimuth streaking, glacier motion, interferometry, offset tracking.

I. Introduction

The free electron density in the ionosphere varies with the activity of the Sun, the Earth magnetic field and atmospheric parameters. Higher electron concentrations and stronger spatial variations occur mainly in polar regions caused by the shape of the Earth magnetic field. The free electrons interact with electromagnetic waves as a dispersive medium, with inverse effects on the phase and group velocities with stronger effects at lower frequencies. From GPS related works there is a good understanding of ionospheric propagation effects. Meyer et al. [1] summarized the theoretical background of ionospheric propagation and evaluated the possibility of measuring ionospheric electron concentrations using a pair of SAR acquisitions, mainly concentrating on interferometric range phase gradients and range registration offsets. Also known for some time, but with less awareness by the SAR and INSAR community, is that electron density fluctuations result in delay phase ramps across the synthetic aperture that can cause significant azimuth positional shifts. In 2000, Gray et al. [2] presented observations of “azimuth streaking” for C-band (Radarsat) and L-band (JERS-1) interferometric pairs, showed that the streaking was correlated with ionospheric activity, explained how the ionospheric phase delay variations could cause these azimuth shifts, and confirmed that larger phase offsets and azimuth shifts are observed at longer wavelengths, with observed azimuth shifts up to several resolution cells at L-band.

At present, ionospheric electron concentration effects on SAR and INSAR are becoming increasingly important on the one hand because of the increased relevance of polar regions studies using SAR data and on the other hand because of the launch of the L-band ALOS PALSAR on 24. January 2006 and the evaluation of further potential L-band systems.

Our work presented in this contribution has a practical background. Using L-band INSAR and offset tracking for arctic glacier motion monitoring [3], we are interested in identifying and, if possible, correcting errors introduced by ionospheric effects. After a short summary of the understanding of the observed effects, the identification of ionospheric anomalies in single SAR scenes as well as for repeat observations is addressed using JERS L-band data. Then modifications to the offset tracking and DINSAR methodologies are proposed to reduce ionospheric anomalies.

II. Ionospheric effects on SAR and INSAR

The ionospheric phase shift for 2-way propagation is [2]:

$$\delta\phi = 1.69 \cdot 10^{-6} N[m^{-2}] \,/\, f[Hz] \qquad (1)$$

where N is the number of electrons per m^2 and f the SAR carrier frequency. A relatively strong change of the free electron density by 1 TECU (= 1. $10^{16}m^{-2}$) results in 2-way range variations of approx. 2.0 phase cycles at L-band, approx. 0.5 phase cycles at C-band, and approx. 0.3 phase cycles at X-band. Spatial changes in the free electron density within a synthetic aperture cause varying phase delays. In the azimuth compression this results in a defocusing in azimuth direction. If the distortion acts as an azimuth phase ramp there results an azimuth positional offset. In real L-band data over polar regions such azimuth offsets of up to several SLC pixels were observed [2]. Another effect, Faraday rotation, is relevant for polarimetry, but can also reduce the interferometric coherence [4] by changing the observed polarization.

Due to the elevation of the ionosphere, the part which affects SAR data is not located vertically above the imaged area but many kilometers towards the satellite sub-track. Due to the side-looking SAR imaging geometry the ionosphere above a given ground location will influence different slant ranges of a SAR image which explains the observed azimuth streaking.

For a single SAR image ionospheric anomalies (i.e. spatial variations in the free electron density) can cause defocusing in the azimuth dimension and azimuth positional shifts. The positional shifts are relevant in geocoding the SAR data or when co-registering two SAR scenes. The latter is of course relevant for SAR interferometry (poor co-registration causing decorrelation) and offset tracking (presence of ionospheric azimuth offsets which are not related to ground surface movements).

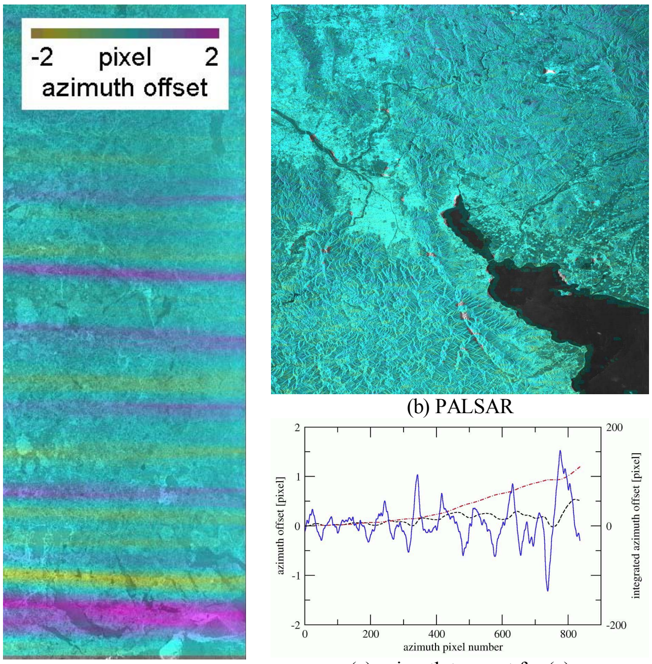

(b) PALSAR

(a) JERS (c) azimuth transect for (a)

Figure 1. Single SLC sub-look azimuth offset fields for JERS-1 data of 11-Dec-1997 over arctic ocean north of Svalbard (a) and ALOS PALSAR data of 21-Mar-2006 over Kyoto, Japan (b), and azimuth transect for image (a) showing azimuth offsets (blue), single integration (black) and double integration (red). The red curve in (c) corresponds to a relative electron density along the transect (arbitrary units).

III. Identification of ionospheric anomalies

A. Single SAR acquisition

Ionospheric anomalies can be detected in a single SAR acquisition by determining the range and azimuth offset fields between azimuth-look images. The peak of the ionospheric electron concentration is roughly located at 200 km to 400 km height, which is a significant fraction of the sensor height. Depending on the squint angle a phase delay located at this height is effective for different ground pixels. Particularly interesting is the azimuth positional offset generated by azimuth phase gradients because this effect is strong and it can be determined even for the pair of interferometrically uncorrelated azimuth sub-look images. An example of an observed sub-look azimuth offset field is shown in Figure 1a. In this example the good contrast of the sea ice permits a complete spatial coverage and high accuracy. Under the condition of sufficient image contrast the azimuth offsets permit reliable identification of ionospheric anomalies within a single SAR acquisition. The processing steps include band-pass filtering of the SLC to get two azimuth sub-look images followed by measuring an offset field between these two sub-look images using a “feature tracking” algorithm that does not depend on coherence [5,6]. This approach can operationally be applied for the detection and localization of ionospheric anomalies, e.g. in JERS-1 or ALOS PALSAR data processing. Applied to the PALSAR sample data made available by JAXA at http://www.eorc.jaxa.jp/ALOS/doc/sproduct.htm no significant sub-look azimuth offsets > 0.3 pixel were identified.

Azimuth offsets are proportional to the azimuth slope of the ionospheric electron density. The observed sub-look azimuth offsets are differences between two images with slightly different squint angles and correspond therefore to the second derivative of the electron density. Double integration of the measured offsets permits calculating a quantity which is proportional to the relative electron density. Unknown integration constants, inaccuracies in the estimated offsets and spatial gaps in the azimuth offset field may prevent getting a quantitative measure of the electron density. An azimuth transect and the corresponding single and double integrations are shown in Figure 1c.

B. Repeat observation pair

As was shown in the past [2] ionospheric anomalies become obvious when calculating an offset field between a repeat orbit SAR data pair as “streaking” in the azimuth offset field. Considering that the phase delays occur not at ground level, but at a height that is a significant fraction of the sensor height it is expected that the ionospheric azimuth offsets depend on the processed bandwidth. Processing for each image of the pair 80%, 40% and 20% of the bandwidth (centered around the Doppler centroid) resulted in the offset fields shown in Figure 2. The general trends observed and locations of positive and negative azimuth offsets are comparable for the three offset fields. Nevertheless, variations become more immediate (better focused) and maximum values significantly higher for lower bandwidths. When processing for each image of the pair only a fraction of the total available azimuth bandwidth the resulting azimuth offset field depends on which part of the spectrum was selected. Figure 3 shows results obtained using each time 20% of the azimuth bandwidth but each time corresponding to different parts of the available bandwidth. The positions of the streaks clearly depend on the squint angle of the processed bandwidth. The influence of the squint angle on the position of an anomaly can be used to estimate effective heights for the layer that causes the phase offsets. For the strongest anomaly observed in Figure 3 the estimated effective height is 222 km. The changes in the electron concentrations are not in a narrow layer at the effective height, but distributed over a relatively broad range of heights, which is also the reason that the observed anomalies are usually long azimuth streaks – for different slant ranges the same anomaly is seen at different heights.

The observed azimuth offsets between pairs of observations correspond to the differences between the azimuth slopes of the ionospheric electron density during the two acquisitions. Single integration in azimuth direction of the measured azimuth offsets permits calculating a quantity which is proportional to the relative change of the electron concentration between the first and second acquisition. Unknown integration constants, inaccuracies in the estimated offsets and spatial gaps in the azimuth offset field complicate the inversion. Furthermore, the side-looking imaging geometry is not ideal to map the ionospheric electron concentration which has a significant vertical depth. Finally, it has to be kept in mind that the location of the observed anomalies is not above the ground location shown in the SAR image, but shifted about 50*km* to 350*km* towards the satellite sub-track, depending on the elevation of the anomaly. A relative electron concentration change map is shown in Figure 2f.

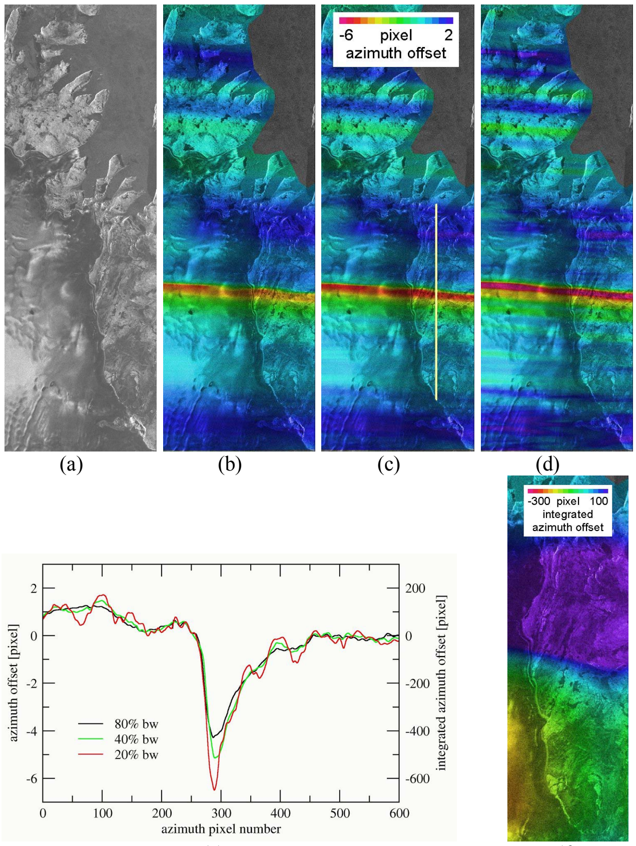

Figure 2. SAR intensity (a), azimuth offset fields between JERS-1 SAR acquisitions of 11-Nov. 1997 a nd 24-Jan-1998 over Svalbard considering 80% (b), 40% (c) and 20% (d) of the azimuth bandwidth, and related profiles across the indicated transect (e), and relative electron concentration map (arbitrary units) of a sub-section obtained by integration of the azimuth offsets of (b) in azimuth direction (f).

IV. MODIFICATION TO OFFSET TRACKING METHODOLOGY

Offset tracking procedures without consideration of ionospheric effects are described in [5,6]. There are important differences between offsets related to ground surface motion and to ionospheric effects that can be used to separate the two effects. Ionospheric anomalies are clearly visible in the azimuth offset field but hardly visible in the range offset field. Furthermore, the typical azimuth streaking geometry of ionospheric azimuth offsets differs from the more localized motion fields of glaciers. To estimate the ionospheric part of the azimuth offsets we first reject azimuth offset estimates for areas with significant (e.g. > 0.2 pixel) range offsets. Furthermore, estimates over specific areas of interest (e.g. glaciers) are rejected. Then the remaining azimuth offset field is filtered and interpolated taking into account the strong directionality of the azimuth streaks by using filters and interpolators that are significantly longer in the range direction than in the azimuth direction. Finally, this ionospheric azimuth offset estimate is subtracted from the initial offset field (Figure 4). The remaining offsets are interpreted as ground surface movements (Figure 5). Uncompensated ionospheric offsets can be identified by comparison with the ionospheric azimuth offset estimate.

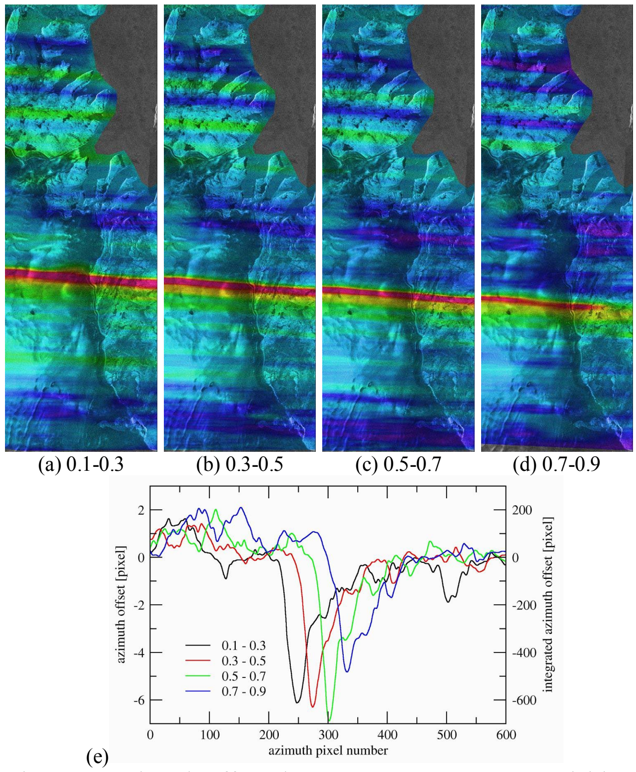

Figure 3. Azimuth offsets between JERS-1 SAR acquisitions of 11-Nov. 1997 and 24-Jan-1998 over Svalbard considering the indicated 20% of the azimuth bandwidth (a-d) and related profiles (e). Color scale, transect location and image size as in Figure 2c. Image size is 40*km* x 120*km*.

V. MODIFICATION TO DINSAR METHODOLOGY

Changes of the ionospheric phase delay within a synthetic aperture cause significant azimuth positional offsets. In SAR interferometry registration errors cause decorrelation of the signal. An example of complete correlation loss due to an ionospheric anomaly is shown in Figure 6. The coherence of the image pair is significantly improved by taking into account the ionospheric offsets determined using offset tracking. For the area of the ionospheric anomaly two full extra phase cycles are observed, most likely caused by the changing phase delay in the ionosphere. In our method we first estimated a registration offset field based on the orbital data and the terrain topography. A large area correction to this accounts for inaccuracies in the orbit geometry. This correction consists of first order polynomials in range and azimuth. Using these offsets the two SLC were co-registered. Deviations from this co-registration are related to surface displacements and ionospheric azimuth offsets. Next, the ionospheric azimuth offsets were determined, as described in Section IV, and added to the previously determined offset field. The slave SLC was then transformed in a single resampling step to the geometry of the master SLC. So far we have not applied any phase correction to compensate the ionospheric effects.

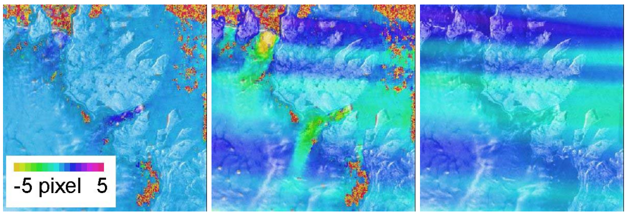

Figure 4. Range (left) and azimuth (center) offsets between JERS-1 SAR acquisitions of 11-Nov. 1997 to 24-Jan-1998. The right image shows the estimated “ionospheric azimuth offsets”.

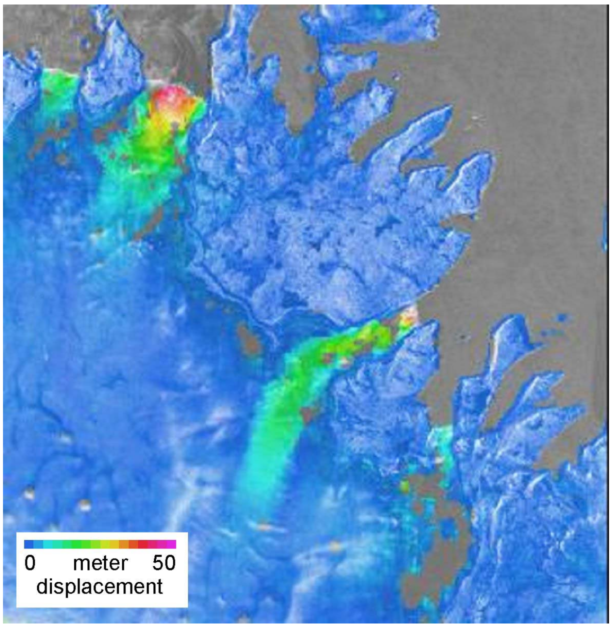

Figure 5. Horizontal displacements at Schweigardbreen and Duvebreen (Austfonna, Svalbard) during the 44-day-period 11-Nov. 1997 to 24-Jan-1998 determined from JERS-1 SAR data using offset tracking techniques and correcting for ionospheric anomalies. Image is in SAR geometry.

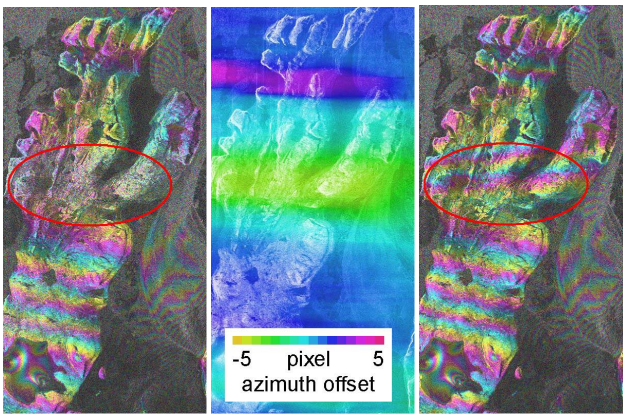

Figure 6. JERS differential interferogram of 23-Mar-1994 and 6-May-1994 ($B_{\perp} = 310m$) before (left) and after (right) correcting the registration for the “ionospheric azimuth offsets” (center). In the area of the strongest anomaly (red ellipse) the coherence improves significantly and two full fringes possibly related to the ionospheric path delay become clearly visible.

VI. Conclusions

The investigated JERS L-band SAR data at high latitudes gives further evidence for the existence and levels of ionospheric effects on SAR. The main effects observed included defocusing in azimuth, positional offsets in azimuth (up to > 5 pixels), and decorrelation and phase effects (up to > 2 fringes) in interferograms. A method to detect ionospheric anomalies in a single SAR acquisition was proposed: Non-zero azimuth offsets between azimuth look images clearly indicated ionospheric anomalies. Applying this methodology can be used to operationally check L-band SAR data for ionospheric anomalies – e.g. in ALOS PALSAR processing. Anomalous azimuth offsets between pairs of repeat-orbit acquisitions are another clear indication for the presence of ionospheric effects. It was shown that ground motion and ionosphere related offsets can often been separated. A modified offset tracking method correcting ionosphere related azimuth offsets was presented and successfully applied. The estimated offset fields were also used to significantly improve the coherence of interferograms in the case of ionospheric anomalies. For the affected areas ionospheric phase effects up to 4π were observed, giving further evidence for the ionospheric origin of the azimuth positional offsets.

The observed ionospheric effects were also used to address the possibility to map electron concentration densities. Information on the location, altitude, and relative electron density change could be derived.

In the L-band SAR scenes and pairs studied we did not find indications of effects from “high electron density tubes”, as simulated in [1,2]. All the strong narrow anomalies identified corresponded to relatively localized changes of the electron density between different electron density levels.

VII. Acknowledgements

Work supported by the FP6 EC INTEGRAL project with Swiss contribution under BBW Nr. 03.0049. JERS SAR data courtesy C1P.2611. DEM of Nordaustlandet © NPI, PALSAR data from http://www.eorc.jaxa.jp/ALOS/doc/sproduct.htm.

VIII. References

[1] Meyer F., R. Bamler, N. Jakowski, and T. Fritz, The potential of broadband L-band SAR systems for small scale ionospheric TEC mapping, Procs. FRINGE 2005 Workshop, Frascati, Italy, 28. Nov. - 2 Dec., 2005 (http://earth.esa.int/workshops/fringe2005).

[2] Gray A.L. D.E. Mattar, and G. Sofko, Influence of ionospheric electron density fluctuations on satellite radar interferometry, Geophys. Res. Letters, Vol. 27, No. 10, pp. 1451-1454, 2000.

[3] Strozzi T., A. Wiesmann, A. Sharov, U. Wegmuller, C. Werner, Capabilities of L-band SAR data for arctic glacier motion estimation, Submitted to IGARSS’2006.

[4] Rignot E., Effect of Faraday rotation on L-band interferometric and polarimetric synthetic aperture radar data, IEEE Trans. Geosci. Remote Sensing, Vol. 38, pp. 2384-2391, 2000.

[5] Strozzi T., A. Luckman, T. Murray, U. Wegmüller, C. Werner, Glacier motion estimation using SAR offset-tracking procedures, IEEE Trans. Geosci. Remote Sensing, Vol. 40, No. 11, pp. 2384-2391, 2002.

[6] Werner C., U. Wegmüller, T. Strozzi, and A. Wiesmann, Precision estimation of local offsets between SAR SLCs and detected SAR images, Proc. IGARSS 2005, Seoul, Korea, 25-29 Jul. 2005.